

Magnetic ordering induced magnetodielectric effect in $Ho_2Cu_2O_5$ and $Yb_2Cu_2O_5$

Hao Jin(金昊), Shuai Huang(黄帅), Kai-Qi Wan(万凯奇), Chang-Ming Zhu(朱长明),Hai-Ou Wang(王海欧), Kun-Peng Su(苏昆朋), and De-Xuan Huo(霍德璇)

Citation: Chin. Phys. B, 2023, 32 (**6**): 067504. DOI: 10.1088/1674-1056/ac904a
Journal homepage: http://cpb.iphy.ac.cn; http://iopscience.iop.org/cpb

What follows is a list of articles you may be interested in

Strong spin frustration and magnetism in kagomé antiferromagnets $LnCu_3(OH)_6Br_3$ (*Ln*=Nd, Sm, and Eu)

Jin-Qun Zhong(钟金群), Zhen-Wei Yu(余振伟), Xiao-Yu Yue(岳小宇), Yi-Yan Wang(王义炎), Hui Liang(梁慧), Yan Sun(孙燕), Dan-Dan Wu(吴丹丹), Zong-Ling Ding(丁宗玲), Jin Sun(孙进), Xue-Feng Sun(孙学峰), and Qiu-Ju Li(李秋菊)

Chin. Phys. B, 2023, 32 (**4**): 047505. DOI: 10.1088/1674-1056/acb9e8

Slight Co-doping tuned magnetic and electric properties on cubic $BaFeO_3$ single crystal

Shijun Qin(覃湜俊), Bowen Zhou(周博文), Zhehong Liu(刘哲宏), Xubin Ye(叶旭斌), Xueqiang Zhang(张雪强), Zhao Pan(潘昭), and Youwen Long(龙有文)

Chin. Phys. B, 2022, 31 (**9**): 097503. DOI: 10.1088/1674-1056/ac7549

Magnetic and magnetocaloric effect in a stuffed honeycomb polycrystalline antiferromagnet $GdInO_3$

Yao-Dong Wu(吴耀东), Wei-Wei Duan(段薇薇), Qiu-Yue Li(李秋月), Yong-Liang Qin(秦永亮),Zhen-Fa Zi(訾振发), and Jin Tang(汤进)

Chin. Phys. B, 2022, 31 (**6**): 067501. DOI: 10.1088/1674-1056/ac43a1

Incommensurate-commensurate magnetic phase transition in double tungstate $Li_2Co(WO_4)_2$

Xiyu Chen(陈西煜), Ning Ding(丁宁), Meifeng Liu(刘美风), Tao Zou(邹涛), V. Ovidiu Garlea, Jingwen Gong(龚婧雯), Fei Liu(刘飞), Yunlong Xie(谢云龙), Lun Yang(杨伦), Shuhan Zheng(郑书翰), Xiuzhang Wang(王秀章), Shuai Dong(董帅), T. Charlton, and Jun-Ming Liu(刘俊明)

Chin. Phys. B, 2022, 31 (**4**): 047501. DOI: 10.1088/1674-1056/ac3818

Strain drived band aligment transition of the ferromagnetic VS_2/C_3N van der Waals heterostructure

Jimin Shang(商继敏), Shuai Qiao(乔帅), Jingzhi Fang(房景治), Hongyu Wen(文宏玉), and Zhongming Wei(魏钟鸣)

Chin. Phys. B, 2021, 30 (**9**): 097507. DOI: 10.1088/1674-1056/ac0cd1

Magnetic ordering induced magnetodielectric effect in $Ho_2Cu_2O_5$ and $Yb_2Cu_2O_5$

Hao Jin(金昊)[1], Shuai Huang(黄帅)[1,2,†], Kai-Qi Wan(万凯奇)[1], Chang-Ming Zhu(朱长明)[2], Hai-Ou Wang(王海欧)[1], Kun-Peng Su(苏昆朋)[1], and De-Xuan Huo(霍德璇)[1,‡]

[1] *Key Laboratory of Novel Materials for Sensor of Zhejiang Province, Institute of Material Physics, Hangzhou Dianzi University, Hangzhou* 310018, *China*
[2] *Guangxi Key Laboratory of Nuclear Physics and Nuclear Technology, Guangxi Normal University, Guilin* 541004, *China*

(Received 24 May 2022; revised manuscript received 2 September 2022; accepted manuscript online 8 September 2022)

Materials with strongly coupled magnetic and electronic degrees of freedom provide new possibilities for practical applications. In this paper, we have investigated the structure, magnetic property, and magnetodielectric (MD) effect in $Ho_2Cu_2O_5$ and $Yb_2Cu_2O_5$ polycrystalline samples, which possess a non-centrosymmetric polar structure with space group $Pna2_1$. In $Ho_2Cu_2O_5$, Ho^{3+} and Cu^{2+} sublattices order simultaneously, exhibiting a typical paramagnetic to antiferromagnetic transition at 13.1 K. While for $Yb_2Cu_2O_5$, two magnetic transitions which originate from the orderings of Yb^{3+} (7.8 K) and Cu^{2+} (13.5 K) sublattices are observed. A magnetic field induced metamagnetic transition is obtained in these two cuprates below Néel temperature (T_N). By means of dielectric measurement, distinct MD effect is demonstrated by the dielectric anomaly at T_N. Meanwhile, the MD effect is found to be directly related to the metamagnetic transition. Due to the specific spin configuration and different spin evolution in the magnetic field, a positive MD effect is formed in $Ho_2Cu_2O_5$, and a negative one is observed in $Yb_2Cu_2O_5$. The spontaneous dielectric anomaly at T_N is regarded as arising from the shifts in optical phonon frequencies, and the magnetoelectric coupling is used to interpret the magnetic field induced MD effect. Moreover, an H–T phase diagram is constructed for $Ho_2Cu_2O_5$ and $Yb_2Cu_2O_5$ based on the results of isothermal magnetic and dielectric hysteresis loops.

Keywords: magnetic ordering, metamagnetic transition, magnetodielectric effect

PACS: 75.47.Lx, 75.85.+t, 77.22.–d, 61.05.cp **DOI:** 10.1088/1674-1056/ac904a

1. Introduction

Multiferroic materials with coexisted ferroelectric and magnetic properties have been widely studied because of potential application prospects in spintronic devices. However, combining ferroelectricity and ferromagnetism in one material is still challengeable, as ferroelectric polarization arises from cations with d^0 or s^2 lone pair electron configuration and ferromagnetism arises from cations with partially filled d or f electrons.[1] Additionally, there is a strict symmetry requirement for magnetoelectric (ME) effect in multiferroic materials.[2] Because of these constraints, the number of multiferroic materials are very limited, and it is necessary to explore other forms of ME effect. The magnetodielectric (MD) effect, which is revealed by the change of dielectric polarization in the magnetic field, is usually observed in multiferroic materials, and it has also been found in single phase ferromagnetic (FM) materials without multiferroic property. Thus, exploring the MD effect would provide a certain degree of impetus to understand the intrinsic mechanism of ME effect, and materials with large MD effect may meet the requirement of application. In the past two decades, large MD effect has been discovered in magnetic field induced multiferroic materials,[3,4] and this effect even retains at room temperature.[5–8] However, the drawbacks of these materials which include the extreme low transition temperature and weak MD coupling make them unable to meet the requirements of practical applications, and the physical mechanism of the MD effect has not been clearly explained. In the process of exploring MD materials, it is found that the dielectric constant (ε) in some intrinsic MD materials is sensitive to the spin structure, and large MD effect may occur in materials with magnetic field induced change of spin configuration and spin–phonon coupling.[9,10] Therefore, the study of MD materials with rich spin structures is expected to understand the physical mechanism and obtain large MD effect.

The $R_2Cu_2O_5$ (R = Y, Sc, In, and Tb–Lu) cuprates have attracted great attention due to the multiple exchange interaction paths and complex spin configurations.[11–26] They crystallize in orthorhombic structure with polar space group $Pna2_1$.[11] In the unit cell, both of Cu^{2+} and R^{3+} have two different positions. The Cu_1 and Cu_2 are strongly coupled, forming a zigzag chain along a axis.[9] Pseudo-planes are formed by adjacent chains, and they are separated by the R^{3+}.[13,14] Due to the strong competition between the crystal field and R^{3+}–Cu^{2+} exchange interaction, the magnetic moments of R^{3+} are polarized under the local effective field generated by the ordered Cu^{2+} spins,[17] and the spin arrangement of R^{3+} and Cu^{2+} differs strongly with different R^{3+}.[13,17] In most cases, the Cu^{2+} shows a similar spin arrangement: FM chains parallel to a axis, and FM or antiferromagnetic (AFM) coupling along b axis.[17] Usually, the low temperature magnetic

†Corresponding author. E-mail: huangshuai@hdu.edu.cn
‡Corresponding author. E-mail: dxhuo@hdu.edu.cn

© 2023 Chinese Physical Society and IOP Publishing Ltd

order of Cu^{2+} and R^{3+} sublattices occurs simultaneously, but a second ordering temperature is detected in $Er_2Cu_2O_5$ and $Yb_2Cu_2O_5$.[11] One of the most interesting effects for these cuprates is the metamagnetic transition.[12,13,15] The metamagnetic transition is characterized by a sudden change in magnetization caused by an applied magnetic field. Such transition usually takes place in AFM materials at a critical magnetic field (H_C). Most of the cuprates exhibit one metamagnetic transition, while cuprates with Y and Sc exhibit two transitions, and $Yb_2Cu_2O_5$ has four transitions in pulse magnetic field.[12] As there are fruitful spin configurations and magnetic field induced spin fluctuations, the MD effect is expected in $R_2Cu_2O_5$. Up to date, the MD effect has been investigated in $Y_2Cu_2O_5$ and $Dy_2Cu_2O_5$.[9,23] The ε shows sudden changes in the spin-flop/flip process, and it is analyzed in terms of magnetostriction and magnon–phonon coupling.[9] As the R^{3+} essentially changes the spin configuration and modifies the characteristic of metamagnetic transition, the dielectric property would be distinctive in the rest $R_2Cu_2O_5$ compounds. In this paper, we have studied the magnetic and dielectric properties in $Ho_2Cu_2O_5$ and $Yb_2Cu_2O_5$ polycrystalline samples. A magnetic ordering induced MD effect is demonstrated, and the possible coupling mechanism is discussed.

2. Experiment

Polycrystalline $Ho_2Cu_2O_5$ and $Yb_2Cu_2O_5$ samples are synthesized by a conventional solid-state reaction method. High purity reagents of Ho_2O_3 (99.999%), Yb_2O_3 (99.999%), and CuO (99.99%) are selected as the starting materials. To obtain the final products, the stoichiometric mixture of the starting materials is pressed into pellets and then heated at 1000 °C for 24 h after intermediate grinding. The crystal structure of the products is checked by using an x-ray diffractometer (XRD, SmartLab, Rigaku) with Cu-K_α radiation. The morphology and elemental analysis are carried out on a scanning electron microscope (SEM, JSM-IT500HR, JEOL) equipped with energy dispersive x-ray spectroscopy (EDX). The magnetization is measured by using a vibrating sample magnetometer (VSM) on a superconducting quantum interference device magnetometer (SQUID, Quantum Design). The ε is measured using a precision LCR meter (E4980AL, Keysight Technologies). The resistivity (ρ) is measured by using a source meter (6517B, Keithley). The magnetic field and the low temperature environment in the ε and ρ measurements are provided by a commercial physical property measurement system (PPMS, Quantum Design). The direction of the magnetic field is set paralleling to that of the electric field.

3. Result and discussion

The powder XRD patterns and the Rietveld refinements for $Ho_2Cu_2O_5$ and $Yb_2Cu_2O_5$ are shown in Figs. 1(a) and 1(b), respectively. High quality of the products is indicated by the small values of the confidence factors ($R_{wp} = 0.0600$, $R_p = 0.0457$, $\chi^2 = 1.8280$ for $Ho_2Cu_2O_5$; $R_{wp} = 0.0578$, $R_p = 0.0424$, $\chi^2 = 2.9480$ for $Yb_2Cu_2O_5$) and the minor difference between the observed and calculated patterns. The results suggest that both samples crystallize in polar orthorhombic structure with space group $Pna2_1$. The obtained lattice parameters are 10.8067(8) Å, 3.4955(7) Å, and 12.4660(5) Å for $Ho_2Cu_2O_5$, and 10.7673(8) Å, 3.4477(4) Å, and 12.3969(1) Å for $Yb_2Cu_2O_5$. These values are in good agreement with previous reported results.[14] Figures 1(c) and 1(d) show the EDX spectra and the corresponding SEM surface morphologies for $Ho_2Cu_2O_5$ and $Yb_2Cu_2O_5$. The atomic ratio of R, Cu, and O is estimated to be 21.98:24.66:53.36 for $Ho_2Cu_2O_5$ and 21.93:24.99:53.08 for $Yb_2Cu_2O_5$, which is close to 2:2:5, indicating the compositional homogeneity.

To give a basic insight of the magnetic behavior for the prepared samples, temperature dependence of magnetization both in zero-field-cooling (ZFC) and field-cooling (FC) modes for $Ho_2Cu_2O_5$ and $Yb_2Cu_2O_5$ with $H = 100$ Oe is measured, and the results are shown in Figs. 2(a) and 2(b), respectively. For $Ho_2Cu_2O_5$, a sharp peak is observed at Néel temperature (T_N) $\sim$ 13.1 K due to that the Ho^{3+} and Cu^{2+} magnetic sublattices order at the same temperature.[11,20] While for $Yb_2Cu_2O_5$, the magnetic ordering of Yb^{3+} and Cu^{2+} sublattices does not occur simultaneously, which is suggested by the two peaks in magnetization curves around $T_{N1} \sim 13.5$ K and $T_{N2} \sim 7.8$ K. The Cu^{2+} sublattices order first at T_{N1}, and the Yb^{3+} sublattices become ordered through a first-order-like transition at T_{N2}. The intermediate transition indicates the competitive and unsatisfied interaction between the Yb^{3+} and Cu^{2+} sublattices.[17] Above T_N, there exists short-range magnetic ordering in these two compounds, leading to the reciprocal susceptibility deviating from linear relation (the data are not shown). To quantitative discuss the magnetic behavior, a nonlinear fitting is performed based on the Curie–Weiss law

$$\chi = C/(T-\theta), \tag{1}$$

where χ is the magnetic susceptibility, C is the Curie constant, and θ is the Weiss temperature. The data far above T_N is selected for the fitting, and the results are shown in Figs. 2(a) and 2(b). The effective magnetic moments (μ_{eff}) are determined to be 13.26 μ_B/f.u. and 5.43 μ_B/f.u. for $Ho_2Cu_2O_5$ and $Yb_2Cu_2O_5$, which are obviously larger than that of free rare earth ion values of Ho^{3+} (10.61 μ_B) and Yb^{3+} (4.54 μ_B), respectively.[18,27] The excess value can be attributed to the magnetic order of the Cu^{2+} (1.98 μ_B) sublattices. The corresponding values of θ are obtained to be -11.2 K and -7.9 K. The negative values of θ indicate the AFM ground state for both compounds. The insets of Figs. 2(a) and 2(b) show the FC curves with various magnetic fields for $Ho_2Cu_2O_5$ and $Yb_2Cu_2O_5$. When the magnetization is recorded with larger magnetic fields, the cusp for the AFM transition is suppressed, and it moves to lower temperature gradually, indicating enhanced paramagnetic property.

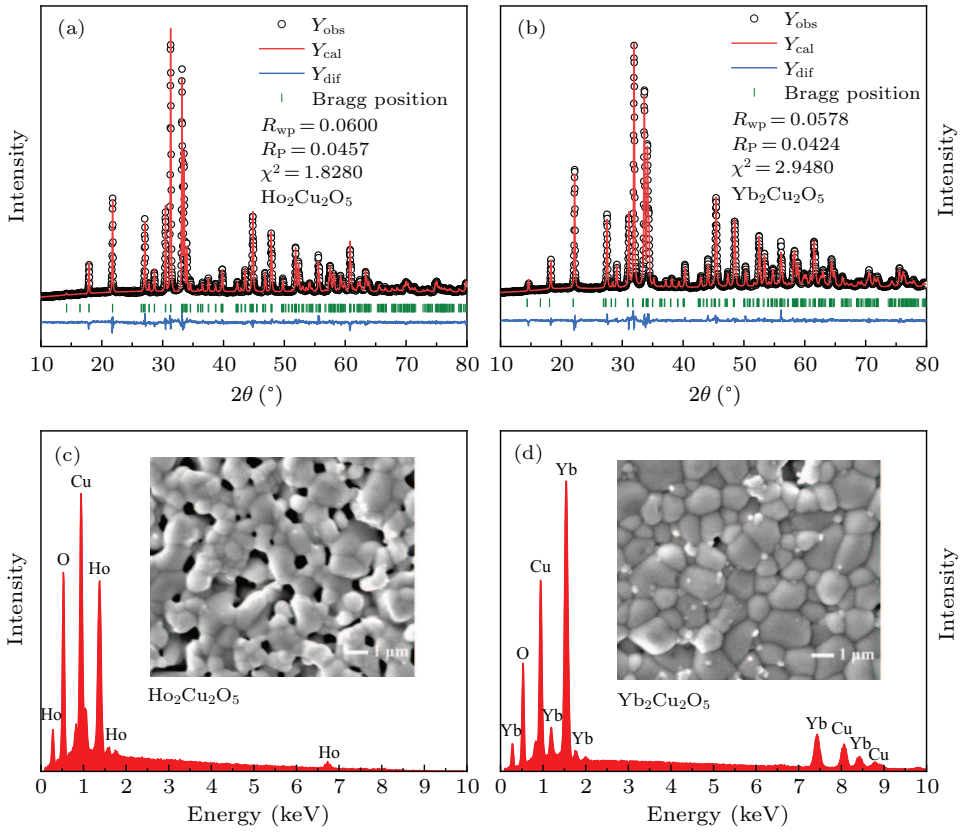


Fig. 1. Room-temperature powder XRD pattens for (a) $Ho_2Cu_2O_5$ and (b) $Yb_2Cu_2O_5$, respectively. The black circles represent the observed data, the red curves are the calculated data, the blue curves indicate the difference between the observed and calculated data, and the green vertical bars indicate the Bragg position. (c) and (d) The EDX spectra for $Ho_2Cu_2O_5$ and $Yb_2Cu_2O_5$. The insets of (c) and (d) show the SEM surface morphology.

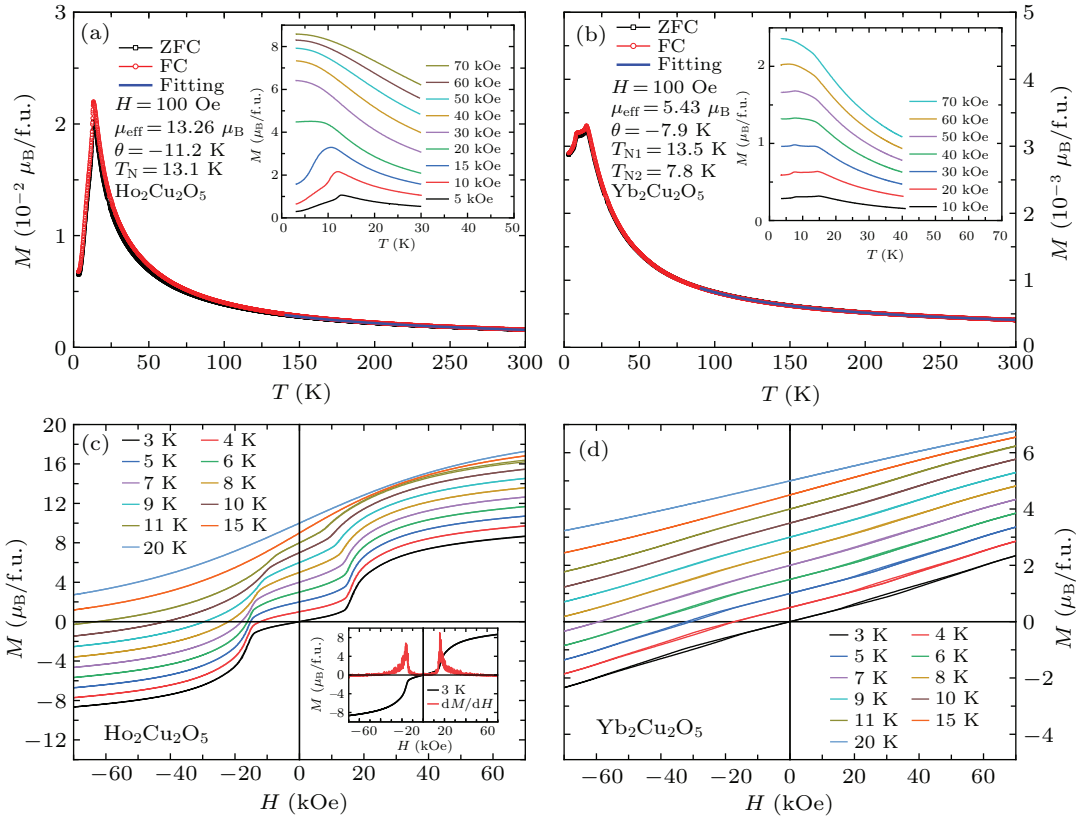


Fig. 2. Temperature dependence of ZFC and FC magnetization for (a) $Ho_2Cu_2O_5$ and (b) $Yb_2Cu_2O_5$ with $H = 100$ Oe, respectively. The blue curves indicate the nonlinear Curie–Weiss fitting. The insets of (a) and (b) show the FC curves with various magnetic fields. (c) and (d) The isothermal magnetic hysteresis loops for $Ho_2Cu_2O_5$ and $Yb_2Cu_2O_5$ at different temperatures. For clarity, the curves are shifted upward except for the loops with $T = 3$ K. The inset of (c) shows the representative curve measured at 3 K, and the red line shows the dM/dH curve.

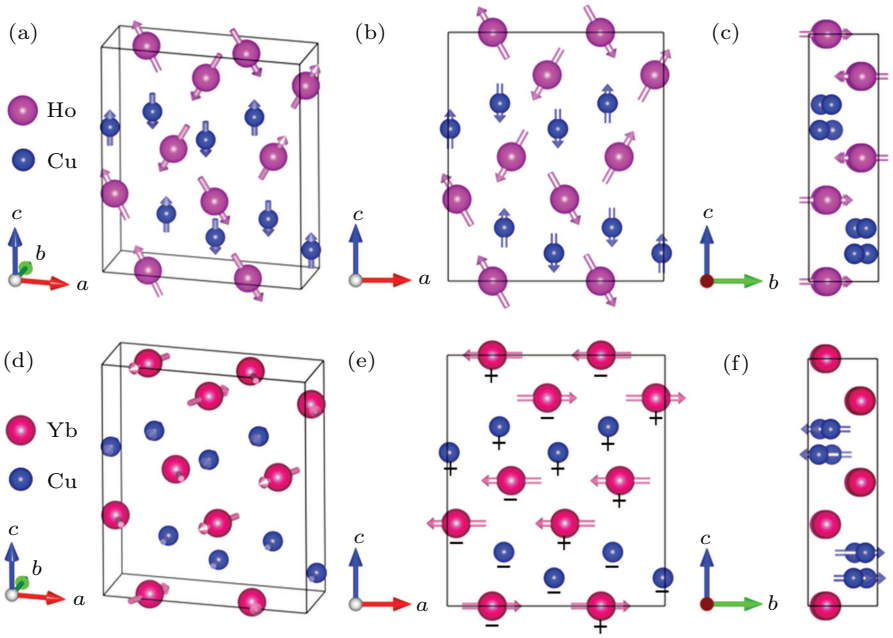


Fig. 3. The magnetic structures and their projections onto *ac* and *bc* planes for (a)–(c) $Ho_2Cu_2O_5$ and (d)–(f) $Yb_2Cu_2O_5$. In the *ac* projections, the directions of the moments are represented. In the *bc* projections, only *y* components of moments are shown. The symbols of + and − indicate the orientations of the moments in *ac* plane. Spins in adjacent cells are inverted according to the propagation vector $\boldsymbol{k} = (0, 1/2, 0)$ for $Ho_2Cu_2O_5$ and $\boldsymbol{k} = (0, 1/2, 1/2)$ for $Yb_2Cu_2O_5$.

Figures 2(c) and 2(d) show the magnetic hysteresis loops for $Ho_2Cu_2O_5$ and $Yb_2Cu_2O_5$, respectively. For $Ho_2Cu_2O_5$, the magnetization increases linearly with the increase of magnetic field at first, and a steep jump in magnetization is observed at H_C, suggesting magnetic field induced metamagnetic transition. The value of H_C obtained from the maximum value of dM/dH curve approaches 16 kOe at 3 K [inset of Fig. 2(c)]. With increasing temperature, it decreases gradually. Above T_N, the H_C becomes indistinguishable, and nonlinear hysteresis loops are observed due to the short-range magnetic ordering. At the maximum magnetic field of 70 kOe, no saturation of magnetization is achieved. For $Yb_2Cu_2O_5$, the field induced metamagnetic transition can also be found, but regular metamagnetic feature of slop change is observed [Fig. 2(d)]. The metamagnetic transition indicates that some of the AFM exchange interaction is suppressed by the external magnetic field in these cuprates. In the simplest case, the spin-flip/flop of Cu^{2+} along *b* axis is response for the metamagnetic transition in $Y_2Cu_2O_5$.[12,13] For $R_2Cu_2O_5$ with magnetic R^{3+}, the spin evolution becomes complex. To understand the metamagnetic transition for $Ho_2Cu_2O_5$ and $Yb_2Cu_2O_5$, the magnetic structures and their projections onto *ac* and *bc* planes are given in Figs. 3(a)–3(c) and 3(d)–3(f) based on the neutron diffraction data in Ref. [17]. Below T_N, it is reported that $Ho_2Cu_2O_5$ appears to be commensurate with the crystal lattice, having propagation vectors $\boldsymbol{k} = (0, 1/2, 0)$, and the magnetic cell is doubled along *b* axis.[20] The Ho^{3+} moments in the same *ab* plane are basically AFM coupled, and the moments in adjacent Ho^{3+} planes are noncollinear.[17] As shown in Fig. 3(c), the spin flip of *y* components of Ho^{3+} moments is more likely to induce the metamagnetic transition in the hysteresis loop below T_N. Similar behavior is also found in $Er_2Cu_2O_5$, in which the field induced metamagnetic transition results from the flip of m_y components of Er atoms.[17] For $Yb_2Cu_2O_5$, the neutron diffraction data suggest that it possesses a low temperature magnetic structure with a propagation vector $\boldsymbol{k} = (0, 1/2, 1/2)$, and the moments of Cu^{2+} in $Yb_2Cu_2O_5$ keep the same arrangement with that in $Y_2Cu_2O_5$ but the spins are inverted in neighbor cells along *b* and *c* axes.[17] It should note that the metamagnetic transition remains above T_{N2}, and it disappears above T_{N1} in $Yb_2Cu_2O_5$ [Fig. 2(d)]. Thus, the spin-flop/flip of Cu^{2+} moments along *b* axis maybe response for the metamagnetic transition in $Yb_2Cu_2O_5$ [Fig. 3(f)].

To evaluate the dielectric property, temperature dependence of ε with various magnetic fields for $Ho_2Cu_2O_5$ and $Yb_2Cu_2O_5$ is measured at low temperatures, and the results are shown in Figs. 4(a) and 4(b). For $Ho_2Cu_2O_5$, a spontaneous anomaly in ε–T curves is observed at 13.1 K, and this temperature is in accordance with the AFM ordering temperature, suggesting distinct MD effect. With the increase of the magnetic field, the transition moves to lower temperature, and the anomaly is depressed gradually. For $Yb_2Cu_2O_5$, similar behavior in the ε–T curves is observed, excepting that a broad dielectric peak is observed between T_{N1} and T_{N2} [Fig. 4(b)]. The broad dielectric peaks may arise from the different magnetic ordering temperature of Yb^{3+} and Cu^{2+}. The insets of Figs. 4(a) and 4(b) show the temperature dependence of ε with different frequencies. It is obvious that the anomaly in ε is independent with the measurement frequency, and the dielectric relaxation is ruled out in this temperature region. It should

note that the dielectric anomaly does not originate from ferroelectric polarization by means of pyroelectricity measurements (the data are not shown here). Two physical mechanisms are usually used to interpret the spontaneous dielectric anomaly at the magnetic ordering temperature. The first one is the magnetostriction effect, which leads to the variation of lattice parameter during the magnetic transition.[28] The changed lattice gives rise to an increase or decrease in phonon energies of modes, and ε will be changed according to the Lyddane–Sachs–Teller (LST) formula $\varepsilon_0/\varepsilon_\infty = \omega_L^2/\omega_T^2$, where ε_0 and ε_∞ are the permittivity at zero frequency and optical permittivity, ω_L^2 and ω_T^2 are the long-wavelength longitudinal and transverse optical-phonon mode frequencies, respectively.[10] The second one is the direct magnon–phonon coupling. In this case, the phonon frequency (ω) can be affected by the spin-correlation according to the equation $\omega = \omega_0 + \lambda\langle S_i \cdot S_j\rangle$, where ω_0 is the phonon frequency in the case of absent spin–phonon coupling, and λ is the coupling constant.[29] Based on the LST formula, ε would be modified.[10] Further studies such as Raman scattering are needed to provide a more complete understanding of the dielectric anomaly in present samples.

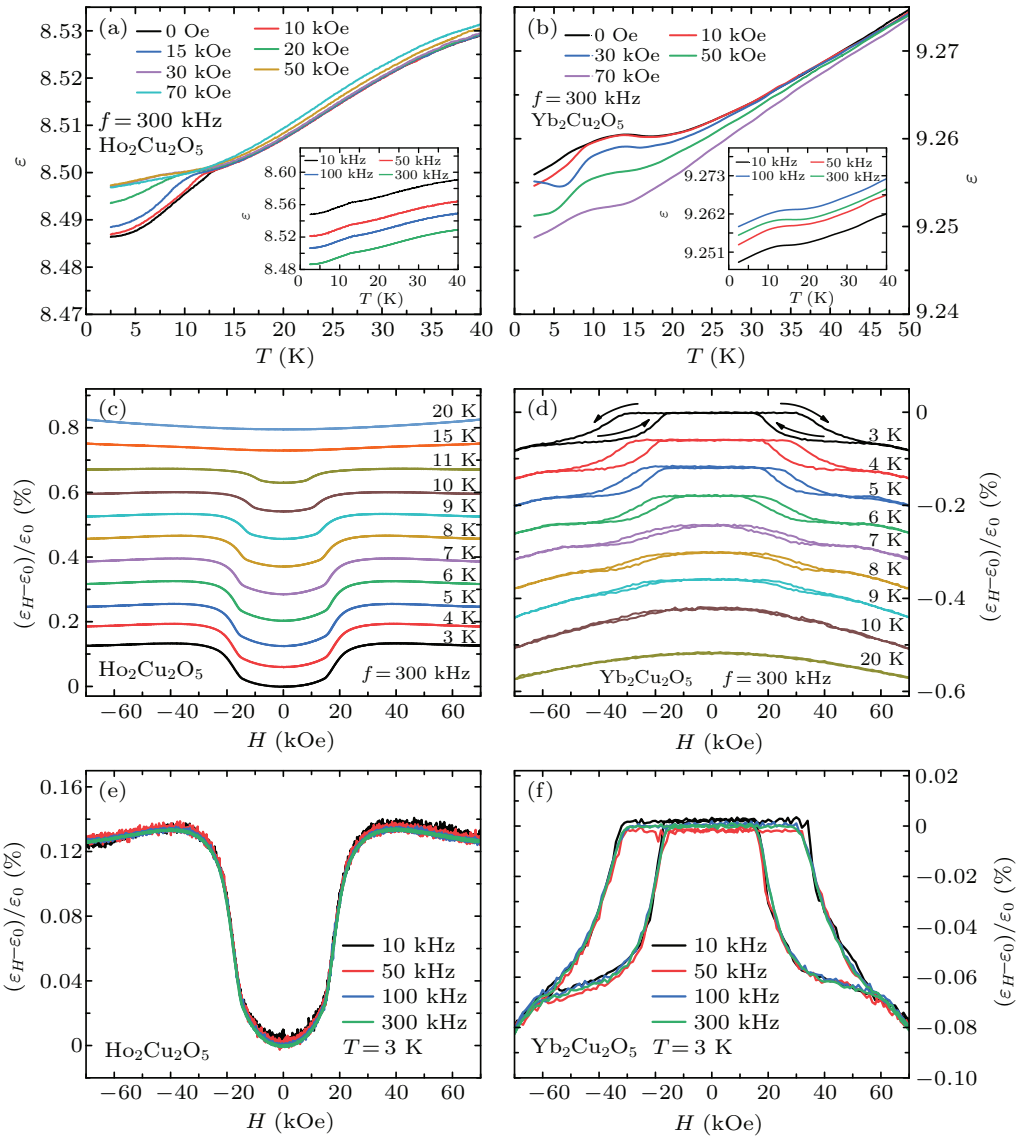


Fig. 4. Temperature dependence of ε with various magnetic fields with the measurement frequency of 300 kHz for (a) $Ho_2Cu_2O_5$ and (b) $Yb_2Cu_2O_5$, respectively. The insets of (a) and (b) show the ε with different frequencies. (c) and (d) The magnetic field dependence of MD coupling parameter with the measurement frequency of 300 kHz for $Ho_2Cu_2O_5$ and $Yb_2Cu_2O_5$, respectively. For clarity, the curves are shifted upward except for the data with $T = 3$ K. (e) and (f) The magnetic field dependence of MD coupling parameter with measurement frequencies of 10 kHz, 50 kHz, 100 kHz, and 300 kHz at 3 K for $Ho_2Cu_2O_5$ and $Yb_2Cu_2O_5$, respectively.

To further investigate the character of MD effect, the magnetic field dependence of ε is measured at various temperatures, and the results are shown in Figs. 4(c) and 4(d). The calculated MD coupling parameter is defined as MD = $(\varepsilon_H - \varepsilon_0)/\varepsilon_0$, where ε_H is the ε in the presence of a magnetic field, and ε_0 is the ε without magnetic field. For clarity, the curves are shifted upward except for the data with $T = 3$ K. For $Ho_2Cu_2O_5$, ε initially increases with the increase of mag-

netic field. After that, a dramatic increase in ε is observed at H_C below T_N. Eventually, ε tends to be stable. The H_C gets smaller with the increase of temperature, and a positive MD effect is formed in the entire temperature range. While for $Yb_2Cu_2O_5$, a completely different MD effect is observed. As shown in Fig. 4(d), ε remains stable with small magnetic field, and it decreases suddenly at H_C. An obvious hysteresis is observed in the MD curves. The variation of H_C is similar with that in $Ho_2Cu_2O_5$, but a negative MD effect is formed. The type of MD effect exhibits close correlation with the rare earth ions and the spin configuration. Based on the magnetic structures data, we have concluded that the spin flip of y components of Ho^{3+} moments and the spin-flop/flip of Cu^{2+} moments along b axis are response for the metamagnetic transition in $Ho_2Cu_2O_5$ and $Yb_2Cu_2O_5$, respectively. The different magnetic ordering induced dielectric anomalies in these two compounds may lead to this different MD properties. To study the influence of measurement frequency on the MD effect, the magnetic field dependence of MD coupling parameter with frequencies of 10 kHz, 50 kHz, 100 kHz, and 300 kHz is measured, and the data for $Ho_2Cu_2O_5$ and $Yb_2Cu_2O_5$ at 3 K are shown in Figs. 4(e) and 4(f), respectively. It is obvious that the data measured with different frequencies almost overlap together for $Ho_2Cu_2O_5$ and $Yb_2Cu_2O_5$ samples, indicating that the MD coupling parameter is independent with the measurement frequency. In multiferroic materials, the MD effect can be understood in terms of magnetoelectric coupling effect.[30,31] The free energy (F) of multiferroics under electric field (E) and magnetic field (H) can be expressed as

$$F = (1/2\varepsilon_0)P^2 - PE - \alpha PM + \beta PM^2 + \gamma P^2M^2, \quad (2)$$

where ε_0 is the bare permittivity, α, β, and γ are the coupling constants, P and M are the polarization and magnetization, respectively.[32,33] As the ferroelectric polarization is excluded by the pyroelectricity measurement, we can just focus on the term γP^2M^2, which solely gives rise to the MD effect. ε can be determined by taking the second derivative of F concerning P, and it should be proportional to γM^2. We have plotted the MD coupling parameter as a function of M^2 and find that all the curves deviate from linear relation. This may be due to the abrupt change of magnetization at H_C. Lawes *et al*. have pointed that the expression of Eq. (2) is not sufficient to describe the MD coupling in AFM materials, and they suggested that γP^2M^2 can be replaced by $\Sigma_q g(q)P^2\langle M_qM_{-q}\rangle$, where $\langle M_qM_{-q}\rangle$ is the q dependent magnetic correlation function, and $g(q)$ is the spin–lattice coupling constant.[29,33] ε is given by $\varepsilon = \varepsilon_0/[1 + 2\varepsilon_0\Sigma_q g(q)\langle M_qM_{-q}\rangle]$.[29] In this model, the q-dependent spin–spin correlations change the value of ε. Using the anomaly transition points in the magnetic and dielectric measurements, we have constructed an H–T phase diagram for $Ho_2Cu_2O_5$ and $Yb_2Cu_2O_5$, and the results are shown in Fig. 5. Below T_N, the phase boundary derived from the distinguishable results in Figs. 2(c), 2(d) and 4(c), 4(d) almost overlaps. It means that the dielectric anomaly is directly related to the metamagnetic transition. We note that the MD effect still exists above T_N, which may arise from the short-range magnetic ordering in these two compounds. The dielectric loss ($\tan\delta$) in this range is less than 10^{-3}. Additionally, ρ increases with the decrease of temperature and reaches up to 10^{10} Ω·m in the measurement accuracy, and no magnetoresistance effect is observed (see Fig. S1 in supplementary material for details). These insulating properties further indicate the intrinsic MD effect in present samples.[34]

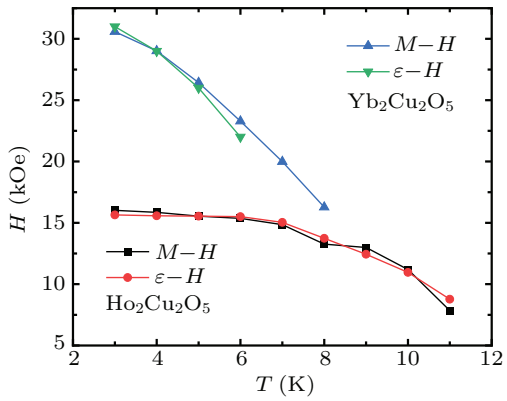


Fig. 5. The H–T phase diagram of $Ho_2Cu_2O_5$ and $Yb_2Cu_2O_5$. The data are derived from the isothermal magnetic and dielectric hysteresis loops.

4. Conclusion

We have investigated the structure, magnetic property, and MD effect in $Ho_2Cu_2O_5$ and $Yb_2Cu_2O_5$. In $Ho_2Cu_2O_5$, Ho^{3+} and Cu^{2+} sublattices order simultaneously at 13.1 K. While for $Yb_2Cu_2O_5$, two magnetic transitions originated from the orderings of Yb^{3+} (7.8 K) and Cu^{2+} (13.5 K) sublattices are observed. A magnetic field induced metamagnetic transition is found in these compounds. Although the lattice possesses a polar space group, no macroscopic ferroelectric polarization can be detected. By means of dielectric measurement, distinct MD effect is demonstrated by the dielectric anomaly at T_N. Meanwhile, the MD effect is found to be directly related to the metamagnetic transition. Due to the specific spin configuration and different spin evolution in the magnetic field, a positive MD effect is formed in $Ho_2Cu_2O_5$ and a negative one is observed in $Yb_2Cu_2O_5$. The spontaneous dielectric anomaly at T_N is regarded as arising from the shifts in optical phonon frequencies, and the magnetoelectric coupling is used to interpret the magnetic field induced MD effect. Further studies such as the neutron diffraction and Raman scattering are needed to provide a clearer spin evolution in the presence of magnetic field and understand the relation between the spin configuration and the dielectric anomaly.

Acknowledgements

Project supported by the Young Scientists Fund of the National Natural Science Foundation of China (Grant No. 11704091), the Open Project of Guangxi Key Laboratory of Nuclear Physics and Nuclear Technology (Grant No. NLK2021-10), and the Open Project of Key Laboratory of Novel Materials for Sensor of Zhejiang Province, China (Grant No. ZJKLNMS2021010).

References

[1] Ravi S P N, Mishra S and Athinarayanan S 2020 *APL Mater.* **8** 040906
[2] Ramesh R and Martin L W 2021 *Riv. Nuovo Cimento* **44** 251
[3] Kagawa F, Mochizuki M, Onose Y, Murakawa H, Kaneko Y, Furukawa N and Tokura Y 2009 *Phys. Rev. Lett.* **102** 057604
[4] Yin L H, Zou Y M, Yang J, Dai J M, Song W H, Zhu X B and Sun Y P 2016 *Appl. Phys. Lett.* **109** 032905
[5] Subramanian M A, He T, Chen J, Rogado N S, Calvarese T G and Sleight A W 2006 *Adv. Mater.* **18** 1737
[6] Rogado N S, Li J, Sleight A W and Subramanian M A 2005 *Adv. Mater.* **17** 2225
[7] Zhang X, Zhao Y G, Cui Y F, Ye L D, Wang J W, Zhang S, Zhang H Y and Zhu M H 2012 *Appl. Phys. Lett.* **100** 032901
[8] Chandrakanta K, Jena R, Pal P, Abdullah M F, Mohapatra S R, Kaushik S D and Singh A K 2020 *J. Mater. Sci.: Mater. Electron.* **31** 15875
[9] Adem U, Nénert G, Arramel, Mufti N, Blake G R and Palstra T T M 2009 *Eur. Phys. J. B* **71** 393
[10] Samara G A and Scott J F 1977 *Solid State Commun.* **21** 167
[11] Troć R, Klamut J, Bukowski Z, Horyń R and Stępień-Damm J 1989 *Physica B* **154** 189
[12] Kazei Z A, Kolmakova N P, Levitin R Z, Mill B V, Moshchalkov V V, Orlov V N, Snegirev V V and Zoubkova J 1990 *J. Magn. Magn. Mater.* **86** 124
[13] arcía-Muñoz J L G, Rodríguez-Carvajal J, Obradors X, Vallet-Regí M, González-Calbet J and Parras M 1991 *Phys. Rev. B* **44** 4716
[14] García-Muñoz J L and Rodríguez-Carvajal J 1995 *J. Solid State Chem.* **115** 324
[15] Matsuoka Y, Nishimura Y, Mitsudo S, Nojiri H, Komatsu H, Motokawa M, Kakurai K, Nakajima K, Karasawa Y and Niimura N 1998 *J. Magn. Magn. Mater.* **177** 729
[16] Cheong S W, Thompson J D, Fisk Z, Martin K A K and Garcia E 1988 *Phys. Rev. B* **38** 7013
[17] García-Munoz J L, Obradors X and Rodríguez-Carvajal J 1995 *Phys. Rev. B* **51** 6594
[18] Li L, Wang J, Su K, Huo D and Qi Y 2016 *J. Alloys Compd.* **658** 500
[19] Lebech B, Matsuoka Y, Kakurai K and Motokawa M 2005 *Prog. Theor. Phys. Supp.* **159** 222
[20] Golosovsky I V, Plakhty V P, Harchenkov V P, Sharigin S V and Schweizer J 1994 *J. Magn. Magn. Mater.* **129** 233
[21] Banerjee A, Sannigrahi J, Giri S and Majumdar S 2017 *J. Phys.: Condens. Matter.* **29** 115803
[22] Murasik A, Fischer P, Troć R and Bukowski Z 1990 *Solid State Commun.* **75** 785
[23] Huang S, Jin H, Wan K Q, Wang H O, Su K P, Yang D X, Yang L and Huo D X 2022 *J. Appl. Phys.* **131** 054102
[24] Denisov V M, Denisova L T, Chumilina L G and Kirik S D 2013 *Phys. Solid State* **55** 2023
[25] Guo R, You J H, Han F, Li C Y, Zheng G Y, Xiao W C and Liu X W 2017 *Appl. Surf. Sci.* **396** 1076
[26] Aldemir D A 2019 *J Mater. Sci.* **30** 19457
[27] Sundaresan A, Ghosh K, Ramakrishnan S, Gupta L C, Chandra G, Sharon M and Vijayaraghavan R 1994 *Phys. Rev. B* **49** 6388
[28] Khanh N D, Abe N, Matsuura K, Sagayama H, Tokunaga Y and Arima T 2019 *Appl. Phys. Lett.* **114** 102905
[29] Lawes G, Ramirez A P, Varma C M and Subramanian M A 2003 *Phys. Rev. Lett.* **91** 257208
[30] Zhou J P, Zhang Y X, Liu Q and Liu P 2014 *Acta Mater.* **76** 355
[31] Alrub A M 2019 *J. Appl. Phys.* **126** 154102
[32] Kimura T, Kawamoto S, Yamada I, Azuma M, Takano M and Tokura Y 2003 *Phys. Rev. B* **67** 180401
[33] Lawes G, Kimura T, Varma C M, Subramanian M A, Rogado N, Cava R J and Ramirez A P 2009 *Prog. Solid State Chem.* **37** 40
[34] Catalan G 2006 *Appl. Phys. Lett.* **88** 102902